

Effects of vascular endothelial cells on osteogenic differentiation of noncontact co-cultured periodontal ligament stem cells under hypoxia

Y. Wu¹, H. Cao², Y. Yang², Y. Zhou³,
Y. Gu⁴, X. Zhao⁴, Y. Zhang⁵,
Z. Zhao⁶, L. Zhang¹ and J. Yin⁷

¹State Key Laboratory of Oral Diseases, Department of Orthodontics, West China College of Stomatology, Sichuan University, Chengdu, China, ²State Key Laboratory of Oral Diseases, Department of Oral and Maxillofacial Surgery, West China College of Stomatology, Sichuan University, Chengdu, China, ³State Key Laboratory of Oral Diseases, Department of Oral Medicine, West China College of Stomatology, Sichuan University, Chengdu, China, ⁴State Key Laboratory of Oral Diseases, West China College of Stomatology, Sichuan University, Chengdu, China, ⁵West China College of Public Health, Sichuan University, Chengdu, China, ⁶Department of Cardiology, West China Medical School, Sichuan University, Chengdu, China and ⁷State Key Laboratory of Oral Diseases, Department of prosthodontics, West China College of Stomatology, Sichuan University, Chengdu, PR China

Wu Y, Cao H, Yang Y, Zhou Y, Gu Y, Zhao X, Zhang Y, Zhao Z, Zhang L, Yin J. Effects of vascular endothelial cells on osteogenic differentiation of noncontact co-cultured periodontal ligament stem cells under hypoxia. *J Periodont Res* 2013; 48: 52–65. © 2012 John Wiley & Sons A/S

Background and Objective: During periodontitis or orthodontic tooth movement, the periodontal vasculature is severely impaired by chronic inflammation or excessive mechanical force. This leads to a hypoxic microenvironment of the periodontal cells and enhances the expression of various cytokines and growth factors that may regulate angiogenesis and alveolar bone remodeling. However, the role of hypoxia in regulating the communication between endothelial cells (ECs) and osteoblast progenitors during the remodeling and repair of periodontal tissue is still poorly defined. The aim of this study was to investigate the effects of vascular ECs on osteogenic differentiation, mineralization and the paracrine function of noncontact co-cultured periodontal ligament stem cells (PDLSCs) under hypoxia, and further reveal the involvement of MEK/ERK and p38 MAPK pathways in the process.

Material and Methods: First, PDLSCs were obtained and a noncontact co-culture system of PDLSCs and human umbilical vein endothelial cells was established. Second, the effects of different time-periods of hypoxia (2% O₂) on the osteogenic potential, mineralization and paracrine function of co-cultured PDLSCs were investigated. Third, ERK1/2 and p38 MAPK activities of PDLSCs under hypoxia were measured by western blotting. Finally, we employed specific MAPK inhibitors (PD98059 and SB20350) to investigate the involvement of ERK1/2 and p38 MAPK in PDLSC osteogenesis under hypoxia.

Results: We observed further increased osteogenic differentiation of co-cultured PDLSCs, manifested by markedly enhanced alkaline phosphatase (ALP) activity and prostaglandin E₂ (PGE₂) levels, vascular endothelial growth factor (VEGF) release, runt-related transcription factor 2 (Runx2) and Sp7 transcriptional and protein levels and mineralized nodule formation, compared with PDLSCs cultured alone. ERK1/2 was phosphorylated in a rapid but transient manner, whereas p38 MAPK was activated in a slow and sustained way under hypoxia. Furthermore, hypoxia-stimulated transcription and expression of osteogenic regulators (hypoxia-inducible factor-1 α , ALP, Runx2, Sp7, PGE₂ and VEGF) were also inhibited by PD98059 and SB203580 to different degrees.

Yeke Wu, PhD, State Key Laboratory of Oral Diseases, Department of Orthodontics, West China College of Stomatology, Sichuan University, No 14th, 3rd section, Renmin South Road, Chengdu, 610041, China
Tel: +86 28 87333125
Fax: +86 28 87333125
e-mail: wuyekeboy@qq.com

Key words: endothelial cells; hypoxia; mitogen-activated protein kinase; noncontact co-culture; osteoblast differentiation; periodontal ligament stem cells

Accepted for publication May 26, 2012

Conclusion: Further increased osteogenic differentiation and mineralization of co-cultured PDLSCs under hypoxia were regulated by MEK/ERK and p38 MAPK pathways. And the ECs-mediated paracrine of PGE₂ and VEGF may facilitate the unidirectional PDLSC-EC communication and promote PDLSCs osteogenesis.

Hypoxia is a characteristic feature of many human pathologies and has long been known as a prominent component of the microenvironment in solid tumors (1), ischemic cardiovascular disease (2) and bony or soft-tissue injury (3). A hypoxic environment affects cell survival and initiates angiogenesis by a complex and multistep mechanism (1). Endothelial cells (ECs) are the major cell type involved, and are situated at the interface between blood and tissue (4). Periodontal ligament (PDL) is a highly vascularized tissue that lies between the cementum and alveolar bone, and is continuously under mechanical loading from occlusion and mastication (5). During periodontitis or orthodontic tooth movement (OTM), the periodontal vasculature is severely impaired by chronic inflammation in lesions or by the excessive mechanical force, respectively (5,6). This leads to a hypoxic microenvironment of the periodontal cells, primarily ECs, pluripotent mesenchymal precursors and committed osteoblasts (7). Hypoxia-inducible factor-1 α (HIF-1 α), a key transcription factor responding to hypoxia and relating to vascular endothelial growth factor (VEGF) function during periodontitis, was deduced to be expressed in diseased periodontium (8). The inflamed and hypoxic periodontal tissue enhances the expression of various cytokines and growth factors that may regulate angiogenesis and alveolar bone remodeling, including VEGF, interleukin (IL)-1 β , IL-6 and prostaglandin E₂ (PGE₂). (9). Of these, VEGF is the direct target of HIF-1 and stimulates alveolar bone remodeling via its effects on osteoblastic cells and osteoclast precursors (9). Its expression could be induced by inflammatory mediators of PGE₂, and it also facilitates inflammation in the early stages of periodontal disease by increasing vascular permeability (10).

Hypoxia has been confirmed to be implicated in angiogenesis–osteogene-

sis coupling during bone repair (11). Transiently hypoxic microenvironments (as in inflamed periodontal tissue) represent a conditional stem and progenitor cell niche for HIF-1 stabilization (12). Upon the stimulation of HIFs, osteoblasts as well as ECs secrete vast amounts of PGE₂ and VEGF. They act directly on osteoblasts to induce osteogenesis, or alternatively, act on ECs to induce angiogenesis and indirectly promote osteogenesis by increasing the supply of multipotent stem cells, osteogenic growth factors and nutrients to the site of bone regeneration and repair (13). Genetic, biochemical and pharmacological studies have attempted to identify and characterize the factors involved in the crosstalk between ECs of the bone vascular tissue and osteoblast progenitor cells during bone formation and repair (14); however, the role of hypoxia in the regulation of communication between ECs and osteoblast progenitors during the remodeling and repair of periodontal tissue is still poorly defined.

The notion that human PDL contains stem cells that could be used to regenerate periodontal tissue was eventually verified by Seo *et al.* in 2004 (15). These periodontal ligament stem cells (PDLSCs) expressed the mesenchymal stem cell (MSC) markers STRO-1 and CD146, as well as the tendon-specific transcription factor scleraxis (15). Apart from self-renewal properties and multilineage differentiation potential, PDLSCs are observed to differentiate into cementoblast-like cells, adipocytes and collagen-forming cells under defined culture conditions (15,16). When transplanted into immunocompromised rodents, PDLSCs showed the capacity to generate a cementum/PDL-like structure and contribute to periodontal regeneration (15). Thus, PDLSCs, rather than MSCs, are deduced to play a pivotal role in periodontal tissue reconstruction. Never-

theless, previous studies on periodontal tissue engineering often chose MSCs with constant osteogenic activity for use in research. A comprehensive understanding of the osteogenic differentiation of PDLSCs remains poor. As the periodontal remodeling in periodontal tissue engineering or orthodontic treatment relates closely to PDLSCs instead of MSCs, studying the effect of hypoxia on PDLSCs would provide significant clues for elucidating the mechanisms involved.

Stem cells are tightly linked to their niche or microenvironment, which is primarily made up of a specialized vascular bed of ECs and regulates stem-cell behaviors (17,18). Niche cells provide a sheltering environment that protects stem cells from differentiation, apoptosis and other stimuli that would challenge stem-cell reserves. A functional niche can maintain the balance of stem-cell quiescence and activity (19). Several studies also confirmed that PDL from mouse molars contains a slowly dividing population of progenitor cells that is located in perivascular sites (20,21). Alveolar bone remodeling during periodontal regeneration results from the combinational process of both bone resorption and bone formation, which are driven by the activities of osteoblasts and osteoclasts derived from stem cells (22). As the relationship between the vasculature and stem cells has been extensively studied in recent years (23–25), clarification of the regulatory effect of vascular ECs on osteoblast differentiation of PDLSCs would probably contribute to our understanding of the mechanisms of periodontal remodeling.

The aim of the present study was to explore the impact of hypoxia on osteogenic differentiation and mineralization of PDLSCs when noncontact cocultured with vascular ECs; in addition, we investigated, in greater detail, the role of MEK/ERK and p38 MAPK pathways in this process. First,

we investigated the effects of different time-periods (0, 1, 3, 6, 12 and 24 h) of hypoxia (2% O₂) on PDLSC survival, osteogenic potential [alkaline phosphatase (ALP) activity, PGE₂ and VEGF release, and runt-related transcription factor 2 (Runx2) and Sp7 transcription and expression] and mineralized nodule formation. Second, the effect of hypoxia on ERK1/2 and p38 MAPK activities was investigated by western blot analysis. Finally, specific MAPK inhibitors (PD98059 and SB20350) were employed to investigate the involvement of ERK1/2 and p38 MAPK in PDLSC osteogenesis under hypoxia. By elucidating the relationship between vascular ECs and PDLSCs under hypoxia, we could provide a theoretical basis for further understanding the mechanisms involved in periodontal remodeling, and boost the development of novel cell-based therapeutic approaches for periodontal regeneration and repair.

Material and Methods

Samples and cell culture of periodontal ligament cells

Periodontal ligament cells (PDLs) were isolated and cultured according to previously reported protocols, with slight modification (15). Briefly, human premolars and impacted third molars extracted from systemically healthy adults at the Department of Oral and Maxillofacial Surgery in our hospital were used under approved guidelines set by the Institutional Review Board, West China College of Stomatology, Sichuan University. Written informed consent was obtained from all donors.

PDL tissues were separated from the surface of the root and minced. Then, they were digested for 1.5 h at 37°C in α -minimum essential medium (α -MEM; Gibco BRL, Grand Island, NY, USA) containing 3 mg/mL of collagenase type I (Gibco) and 4 mg/mL of dispase (Gibco).

Single-colony selection of PDLSCs

PDLSCs were obtained as previously described (8). Briefly, the digested cells

were passed through a 70- μ m strainer (Falcon; BD Labware, Franklin Lakes, NJ, USA) to obtain single-cell suspensions. Then, the single-cell suspensions (1×10^4 cells) were seeded into 10-cm culture dishes (Costar, Cambridge, MA, USA) containing growth medium of α -MEM supplemented with 10% (v/v) fetal bovine serum (CS; HyClone, Auckland, New Zealand), 100 mM L-ascorbic acid 2-phosphate (Sigma-Aldrich, St Louis, MO, USA), 2 mM L-glutamine, 100 U/mL of penicillin and 100 mg/mL of streptomycin (North China Pharmaceutical Co., Ltd, Shanghai, China), and maintained at 37°C in a humidified atmosphere of 5% CO₂. Finally, colony-forming efficiency and proliferation rate of the cells were assessed to identify putative stem cells.

PDLSCs (1×10^6 cells) were transferred to 25-cm² flasks. Every 3 d the medium was replaced with fresh α -MEM. When the cells reached approximately 80% confluence, they were washed twice with phosphate-buffered saline (PBS) and detached with 0.25% trypsin plus 0.05% EDTA (Sigma) for passage. Cells from passages two to four were used in the following experiments.

Immunocytochemical characterization of PDLSCs

Cell characterization was evaluated by immunostaining PDLSCs cultured to confluence for vimentin, CD146 and STRO-1. Briefly, PDLSCs were fixed in 4% (w/v) paraformaldehyde for 20–30 min, washed three times with PBS and air-dried at 4°C. Then, the PDLSCs were treated with 3% hydrogen peroxide for 15 min at room temperature to block intrinsic peroxidase and washed three times with PBS. Fixed cells were incubated for 1 h at 37°C with primary antibody to vimentin, CD146 or STRO-1 (mouse anti-human; Abcam, Cambridge, UK) or without primary antibody (control). Subsequently, cells were washed in PBS and incubated with biotin-conjugated rabbit anti-mouse IgG (Santa Cruz, CA, USA) for 0.5 h at 37°C. Finally, they were incubated with horseradish peroxidase-labeled strep-

tavidin for 20 min at 37°C. At least five independent experiments were performed, and cultures were examined using a microscope (Nikon, Tokyo, Japan).

Northern blot analysis

Human bone marrow mesenchymal stem cells (BMMSCs) were obtained as described previously (26). Total RNA (15 μ g) from PDLs, PDLSCs and BMMSCs cultures were electrophoresed and then transferred to a nylon membrane. Probe was generated from purified PCR products with scleraxis primers (Table 1) by random labeling with (γ -³²P) deoxycytidine triphosphate (New England Nuclear, Boston, MA, USA) by use of the Stratagene Prime It II labeling kit (Stratagene, CA, USA). After prehybridization in QuickHyb hybridization solution (Stratagene) at 68°C for 15 min, the filters were hybridized with scleraxis probe at 68°C for 1 h. The filters were washed twice in 2 \times standard sodium chloride and sodium citrate solution, containing 0.1% (w/v) SDS, for 15 min at room temperature, followed by one wash in 0.1% standard sodium chloride and sodium citrate solution, containing 0.1% (w/v) SDS, at 68°C for 30 min. The membranes were then exposed to a PhosphoImager cassette (Amersham Bioscience, Sunnyvale, CA, USA) for 16–72 h.

In vivo transplantation of PDLSCs

The animal experiment protocol was approved by the Institutional Animal Care and Use Committee, Sichuan University, Chengdu, China. *In vitro*-expanded PDLSCs were transplanted with ceramic bovine bone subcutaneously into the dorsal surfaces of the 5-wk-old immunocompromised mice, as previously described, and the BMMSCs were used as controls (27). The transplants were recovered at 6–8 wk post-transplantation, fixed with 4% formalin, decalcified with buffered 10% EDTA (pH 8.0) and then embedded in paraffin. Sections were deparaffinized and stained with hematoxylin and eosin.

Table 1. Primers used for real-time PCR and northern blot analysis

| Gene | GenBank | Primer sequences (5'-3') | Fragment size (bp) |
|---------------|--------------|---------------------------------------|--------------------|
| RUNX2 | NM_001015051 | R 5' - GTGAAGACGGTTATGGTCAAGG -3' | 169 |
| | | F 5' - CAGATGGGACTGTGGTTAGTGT -3' | |
| SP7 | NM_152860 | R 5' - CCACTATTTCCCACTGCCTTG -3' | 125 |
| | | F 5' - ACCTACCCATCTGACTTTTGCTC -3' | |
| HIF1 α | NM_000963 | R 5' - CTACCAGAAGGGCAGGATACAG -3' | 165 |
| | | F 5' - GCAGGCAGATGAAATACCAGTC -3' | |
| Scleraxis | BK000280 | R 5' - ACTTGGCCCAGGTAG -3' | 405 |
| | | F 5' - GTCGACCGCCGCCGCCACCAC -3' | |
| GAPDH | NM_002046 | R 5' - GTAGAGGCAGGGATGATGTTCT -3' | 132 |
| | | F | |
| | | 5' - CTTTGGTATCGTGAAGGACTC -3' | |

The primers for runt-related transcription factor 2 (*RUNX2*), *SP7*, hypoxia-inducible factor-1 α (*HIF1 α*) and glyceraldehyde-3-phosphate dehydrogenase (*GAPDH*) were used in RT-PCR, and the primers for *Scleraxis* were used in the northern blot.

F, forward; R, reverse.

Culture of human umbilical vein endothelial cells

Human umbilical vein endothelial cells (HUVECs) were purchased from the American Type Culture Collection (ATCC, Manassas, VA, USA) (ATCC code: CRL-1730). Cells were cultured in α -MEM supplemented with 10% (v/v) fetal bovine serum, 2 mM L-glutamine, 100 U/mL of penicillin and 100 mg/mL of streptomycin. All cells were cultured in 25-cm² flasks and incubated at 37°C in 5% CO₂. Every 3 d the medium was replaced with fresh α -MEM. Upon reaching 80% confluence, the cells were detached with trypsin for subculture.

Establishment of the PDLSCs/HUVECs noncontact co-culture system

Millicell Culture Plate Inserts (Millipore, Billerica, MA, USA), containing polycarbonate membranes with a pore size of 0.4 μ m, were placed in the wells of a six-well culture plate to establish the noncontact co-culture system. Each membrane was seeded with 1×10^5 and 1×10^5 PDLSCs per well in 2.4 mL of

medium were added to the outside of the inserts. Thus, the cell monolayer in the insert and common culture plate was divided by the polycarbonate membrane, while the culture medium could pass through the pores, which had an aperture of 0.4 μ m.

Hypoxic treatment of PDLSCs and noncontact co-cultures

At 95% confluence, PDLSCs at passages two to four were placed in six-well plates at a density of 1×10^4 PDLSCs/cm². The cells or noncontact co-cultures were incubated for 2 d at 37°C in an atmosphere of 5% CO₂, 100% humidity. Then, they were subjected to hypoxia in a modular hypoxic incubator (Binder, Villingen, Germany). The cells were assigned to two groups: the hypoxic group (2% oxygen), divided into five subgroups (1, 3, 6, 12 and 24 h), according to different time-periods of hypoxic exposure; and the normoxic control group (20% oxygen). Cell-culture plates were placed in the incubator and saturated with a gas mixture containing 2% oxygen, 5% CO₂ and 93% nitrogen for the generation of hypoxia at 37°C for

specific periods of time (1, 3, 6, 12 and 24 h). Three replicates were used for each condition, and the experiments were performed at least three times.

Pharmacological MAPK-inhibition study

This pharmacological inhibition study was employed to investigate the function of MEK/ERK and p38 MAPK signals in osteogenesis. Specific inhibitors of MEK/ERK (PD98059) and p38 MAPK (SB20350) were added to the culture medium at the indicated time-points. The minimum effective concentration (MEC) of inhibitors necessary for significant inhibition of kinase phosphorylation was determined by a concentration gradient test, in which PD98059 was used at final concentrations of 5, 10 and 20 μ M, and SB20350 was used at 1, 3 and 9 μ M. The MAPK inhibitors were dissolved in fresh dimethylsulfoxide at a dilution of 1/1000, and were replenished once every 3 d. Control cells were treated with 0.1% dimethylsulfoxide.

ALP assay

PDLSCs in the PDLSCs group or non-contact co-cultured group were fixed and washed twice in PBS. ALP activity was visualized by the incubation of cells in 5-bromo-4-chloroindol-2-yl phosphate/Nitro Blue tetrazolium (BCIP/NBT) (Roche, Mannheim, Germany), as previously reported.

ELISA assays

The amounts of PGE₂ and VEGF protein in the culture supernatant of PDLSCs or in the noncontact co-culture of PDLSCs and HUVECs were measured by ELISA using the Human PGE₂ and VEGF Quantikine ELISA Kit (R&D Systems, Minneapolis, MN, USA), following the manufacturer's instructions. The color intensity was measured at 540 nm in a microtiter plate spectrophotometer. The concentration of protein in the culture medium was determined in triplicate wells and was normalized to standard curves generated for each set of samples assayed.

RNA isolation and quantitative real-time RT-PCR

After hypoxic treatment, cells were washed twice with PBS. Total RNA was extracted using TRIzol (Invitrogen, Camarillo, CA, USA) according to the manufacturer's instructions. Total RNA was quantified, in a spectrophotometer, at an absorbance (A) of 260 nm. The RNA samples had to have an $A_{260} : A_{280}$ ratio of 2.0 to guarantee high purity. Two micrograms of total RNA from each sample was subjected to reverse transcription using the SYBR1 PrimeScript™ RT-PCR Kit (TaKaRa Biotechnology, Dalian, China), according to the manufacturer's instructions. Each real-time PCR amplification was carried out in triplicate in a total reaction mixture of 20 mL (2 mL of cDNA, 10 mL of SYBR1 Premix Ex Taq™, 0.4 mL of ROX Reference Dye II, 0.4 mL of each of 10 mM forward and reverse primers and 6.8 mL of H₂O) in an ABI PRISM 7300 Real-time PCR System (Applied Biosystems, Foster City, CA, USA). The primers used for real-time PCR analysis are presented in Table 1. The PCR program was initiated by a cycle of 1 min at 95°C before 40 thermal cycles, each of 15 s at 95°C, 15 s at 55°C and 1 min at 72°C, were performed. The starting copy numbers of unknown samples were calculated by the 7300 System SDS Software from the standard curve. Each value was normalized to glyceraldehyde-3-phosphate dehydrogenase (GAPDH) as the housekeeping gene to control for variations in the amount of input cDNA. The relative expression levels of the genes were calculated using the $\Delta\Delta C_t$ method and compared with cells of the normoxic control group.

Protein isolation and western blotting

To obtain whole-cell extracts, specimens were collected at specific time-points, washed twice with ice-cold PBS and then lysed and sonicated in lysis buffer (Keygen total protein extraction kit; Keygen Biotech, Nanjing, China). The cytosolic fraction was collected as the supernatant, after centrifugation

(14,000 g , 4°C, 15 min) and assayed quantitatively using the bicinchoninic acid method. After boiling for 5 min, 20–25 μ L of the lysate (50 μ g of protein) was separated by SDS-PAGE (12% polyacrylamide gel) at 120 V for 5 h, and the proteins in the gel were transferred to a polyvinylidene difluoride membrane (Millipore). After blocking, the membranes were probed with 1 : 1000 dilutions of the antibodies to Runx2, Sp7 (diluted 1 : 1000; Abcam, Hong Kong, China) and ERK1/2, p-ERK1/2, p38 MAPK and p-p38 MAPK (diluted 1 : 1000; Cell Signaling, Beverly, MA, USA), overnight at 4°C, followed by the addition of horseradish peroxidase-conjugated secondary antibody (diluted 1 : 5000; Santa Cruz Biotechnology, Santa Cruz, CA, USA) at 37°C for 1 h. Immunoreactive proteins were visualized using a chemiluminescence kit (Immobilon Western Chemiluminescent HRP Substrate; Millipore). Band intensities were determined using the ChemiDoc XRS Gel documentation system and Quantity One software (Bio-Rad, Hercules, CA, USA). The kinase activity was analyzed using the band intensity ratio (Ap-ERK/AERK and Ap-p38 MAPK/Ap38 MAPK).

Mineralized nodule formation assay

Mineralized nodules were assessed using the modified von Kossa's silver nitrate staining method. Briefly, PDLSCs were grown in differentiated medium (Dulbecco's modified Eagle's minimal essential medium/F12 supplemented with 1 μ M dexamethazone and 50 μ g/mL of ascorbic acid) in six-well noncontact co-culture plates under hypoxia for 0, 6, 12, 24, 48 and 72 h. Then, cultures were fixed in cold methanol for 15–20 min. After a rinsing step, the fixed plates were incubated with a 5% silver nitrate solution under ultraviolet light using two cycles of auto-cross-linking (1,200 μ J \times 100) in a UV Stratalinker (Stratagene, La Jolla, CA, USA). Mineralized nodules were seen as dark brown/black spots. The density of mineralized nodules was quantified using Quantity One software (Bio-Rad).

Statistical analysis

All experiments were repeated at least three times and data of evaluation parameters were expressed as mean \pm standard deviation. Statistical comparisons were made using factorial analysis of variance, for comparing treatment groups with controls. $p < 0.05$ was considered as statistically significant.

Results

Cell culture and characterization of PDLSCs

Primary PDLCS were obtained through enzyme digestion method. PDLCS adhered to the wall of the six-well plate on days 5–10 and fused on days 7–14 (Fig. 1A). The putative stem cells obtained by single-colony selection exhibited a typical fibroblast-like spindle appearance and were able to form adherent clonogenic cell clusters (Fig. 1B). Immunocytochemical staining showed that they expressed vimentin (a marker of fibroblasts), STRO-1 and CD146 (two early mesenchymal progenitor markers), which initially suggested that the isolated cells are PDLSCs (undifferentiated mesenchymal stem cells) (Fig. 1B–D).

Then we assessed the expression level of scleraxis, a tendon-specific transcription factor, in PDLCS, PDLSCs and BMMSCs by northern blot analysis. The results demonstrated that PDLSCs expressed a higher level of scleraxis than did BMMSCs ($p < 0.05$), and no significant difference was observed between PDLSCs and PDLCS in expression of scleraxis ($p > 0.05$) (Fig. 2A). In addition to their typical morphology and expression of specific antigens on the cell surface or within the cell, the capacity for osteogenic and adipogenic differentiation of PDLSCs was also evaluated (data not shown).

To validate the putative stem cells from human PDL as PDLSCs, we transplanted *ex vivo*-expanded PDLSCs into immunocompromised mice and verified their capacity to differentiate into PDL-like and cementum-like tissue. A typical cementum/PDL-like

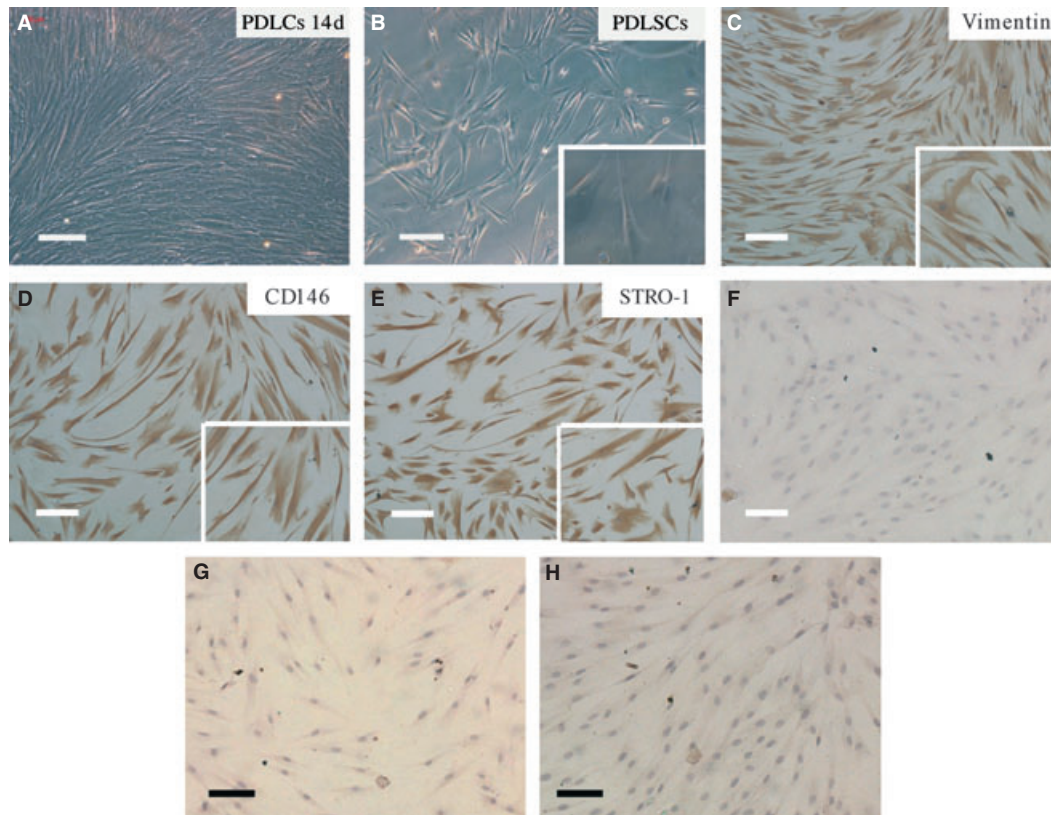


Fig. 1. Morphological observation of periodontal ligament cells (PDLs) and characterization of periodontal ligament stem cells (PDLSCs) by immunocytochemical staining. (A) PDLs adhered to the wall of six-well plate on day 14, assuming a fusiform shape. (B) PDLSCs demonstrate a typical fibroblast-like spindle appearance. The insert is a higher-magnification view ($\times 200$) of the larger image. (C, D, E) Immunocytochemical staining with vimentin (C), CD146 (D) and STRO-1 (E) antibodies. The immunoreactive cells were stained brownish/yellow. The inserts in C, D and E are higher-magnification views ($\times 400$) of the respective images, showing brownish/yellow-stained cytoplasm. (F, G, H) Immunocytochemical staining without vimentin (F), STRO-1 (G) and CD146 (H) primary antibodies, as controls. Scale bars = 100 μm .

structure was regenerated, in which a thin layer of cementum-like tissue formed on the surface of the carrier, along with condensed collagen fibers with sparse cells that resembled PDL structures (Fig. 2B). The cementum/PDL-like structures appeared to be totally different from the typical bone/marrow structures generated by BMMSCs (data not shown).

Sustaining hypoxic treatment augments the ALP activity level in the noncontact co-culture system

To determine the effect of hypoxia on the osteogenic capability of noncontact co-cultured PDLSCs, we measured the ALP activity level in PDLSCs after hypoxic treatment. As shown in Fig. 3A, ALP activity was significantly increased by hypoxia at all time-points compared with the control ($p < 0.05$). During culture, it transiently increased

at 1 h, peaked at 12 h and decreased thereafter, but was still higher than the activity in the control group ($p < 0.05$). The ALP response pattern of the co-cultured PDLSCs was similar to that of PDLSCs under hypoxia. When comparing the co-culture group with the PDLSC group at each time-point, the ALP activity was increased by 2.25-, 1.43-, 1.197-, 1.401-, 2.593- and 1.825-fold, respectively, and the increase was significantly different at all time-points ($p < 0.05$) (Fig. 3A).

Hypoxia promotes further PGE₂ and VEGF release in the noncontact co-culture system

To verify whether hypoxia induces PGE₂ and VEGF release in the noncontact co-culture system of PDLSCs and HUVECs, we initially measured the accumulation of PGE₂ and VEGF in supernatants of the co-cultured

PDLSCs and HUVECs treated with hypoxia, and compared the results with those of the PDLSCs cultured alone under hypoxia. The results showed that PGE₂ secretion was significantly increased at all time-points compared with the control ($p < 0.05$), and peaked at 6h, with a concentration of $96.259 \pm 4.81 \text{ pg}/10^5 \text{ cells/mL}$. When comparing the co-culture group with the PDLSC group at each time-point, the PGE₂ concentration was increased by 1.25-, 1.013-, 1.139-, 1.2-, 1.12- and 1.034-fold, respectively, and was significantly different at 3, 6 and 12 h ($p < 0.05$) (Fig. 3B). Similarly, hypoxia stimulated a significant, sustained enhancement of VEGF release at all time-points compared with the control ($p < 0.05$). Comparison of the co-culture group with the PDLSC group at each time-point showed the VEGF concentration to be increased by 1.27-, 1.35-, 1.25-, 1.32-, 1.28- and

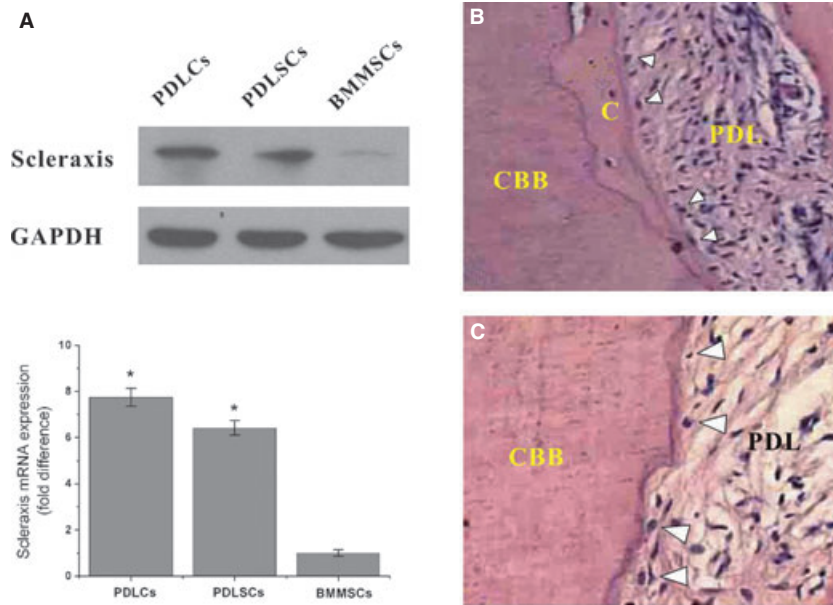


Fig. 2. Scleraxis expression *in vitro* and generation of periodontal ligament (PDL)-like and cementum-like structures *in vivo* by periodontal ligament stem cells (PDLSCs). (A) Northern blot analysis of the scleraxis mRNA level in periodontal ligament cells (PDLs), PDLSCs and bone marrow mesenchymal stem cells (BMMSCs; control). (B) After 8 wk of transplantation, PDLSCs generated PDL-like tissue (PDL), and differentiated into cementoblast-like cells (arrowheads) that formed a cementum-like structure (C) on the surface of the ceramic bovine bone (CBB) carrier (HE staining, $\times 20$). (C) Magnified view of (B) ($\times 40$). $*p < 0.05$ vs. control.

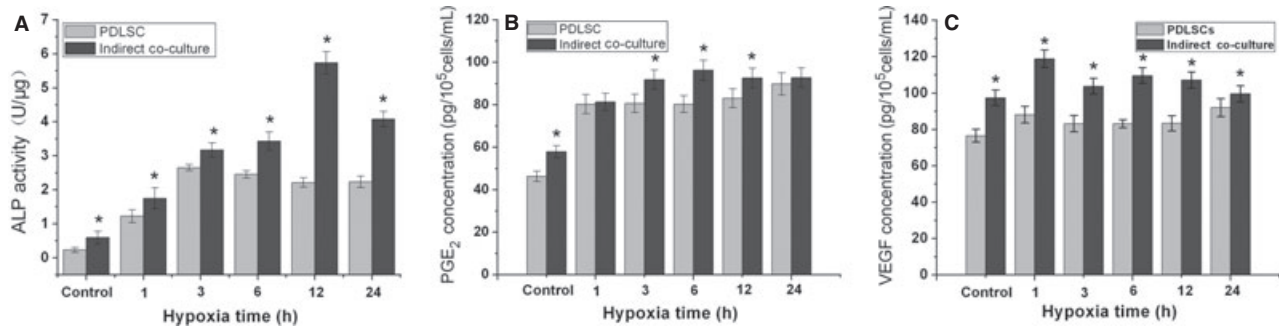


Fig. 3. Alkaline phosphatase (ALP) activity level, and prostaglandin E₂ (PGE₂) and vascular endothelial growth factor (VEGF) concentrations in the supernatant of the noncontact co-cultured periodontal ligament stem cell (PDLSC)/human umbilical vein endothelial cell (HUVEC) system under hypoxic exposure. (A) ALP activity levels of PDLSCs and noncontact co-cultured PDLSCs after various time-periods of hypoxic treatment. (B) Quantification, by ELISA, of PGE₂ released by PDLSCs and by noncontact co-cultured PDLSCs after various time-periods of hypoxic treatment. (C) Quantification, by ELISA, of VEGF released by PDLSCs and by noncontact co-cultured PDLSCs after various time-periods of hypoxic treatment. $*p < 0.05$ between the two groups.

1.08-fold, respectively, and was significantly different at all time-points ($p < 0.05$) (Fig. 3C).

Hypoxia increases the level *RUNX2* and *SP7* mRNAs and expression of Runx2 and Sp7 proteins in the noncontact co-culture system

To understand more clearly the effect of hypoxia on the osteogenic activity of noncontact co-cultured PDLSCs, we

carried out real-time quantitative RT-PCR and western blot experiments to measure the expression levels of *RUNX2* and *SP7* mRNA and Runx2 and Sp7 protein in PDLSCs exposed to different time-periods of hypoxic exposure. The results demonstrated that short-term hypoxic exposure (for 1 h and 3 h) significantly up-regulated the expression of *RUNX2* mRNA compared with the control ($p < 0.05$). The expression of *RUNX2* mRNA

showed a transient increase of about 1.1042-fold at 1 h and peaked at 3 h, then subsequently showed a slight decrease at 6, 12 and 24 h of culture, to levels lower than those of the control group ($p < 0.05$) (Fig. 4A). Comparison of the co-culture group with the PDLSC group at each time-point showed that the *RUNX2* mRNA level was increased by 1.32-, 1.11-, 1.292-, 0.933-, 0.874- and 1.177-fold, respectively, being significantly different at all

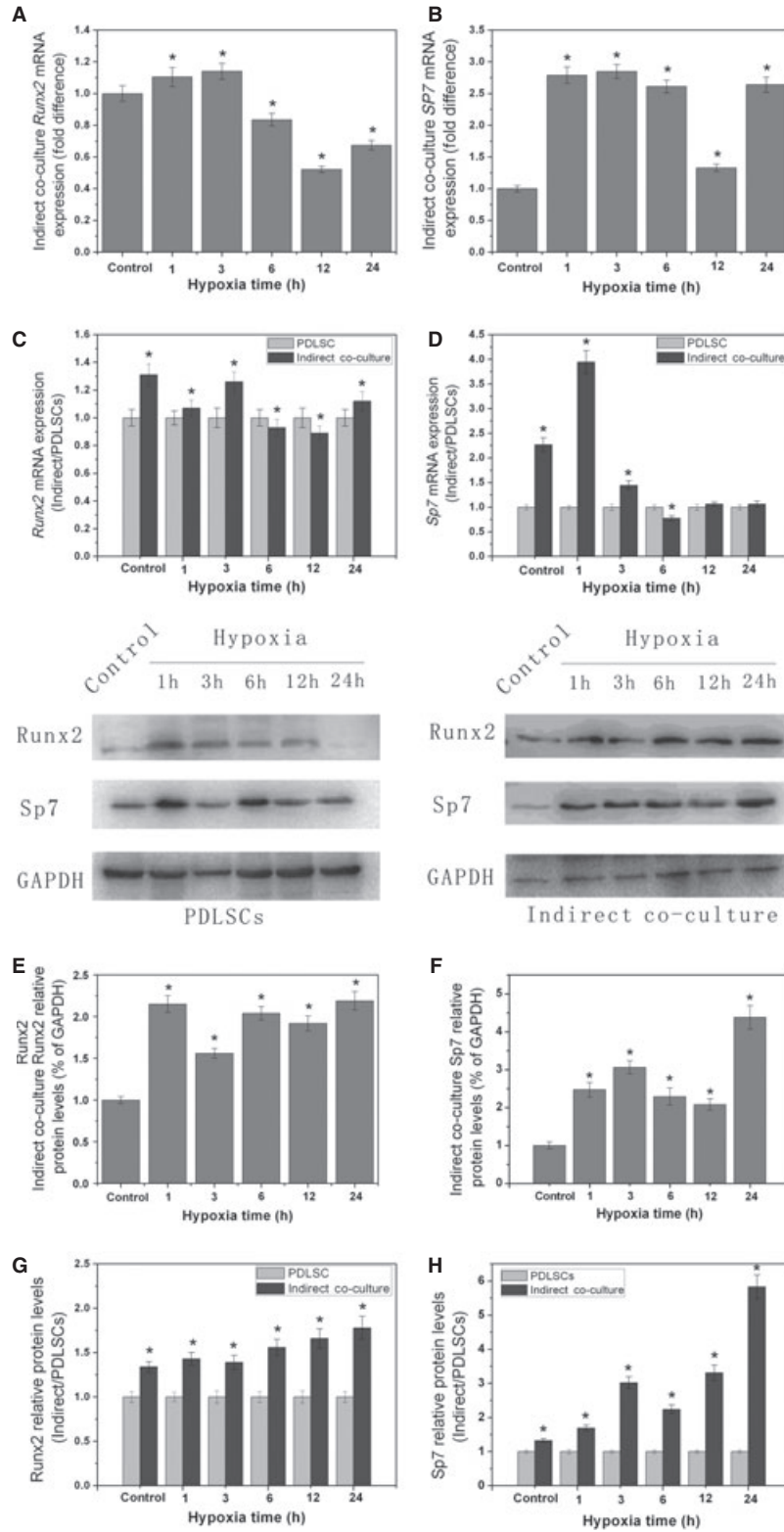


Fig. 4. Expression of runt-related transcription factor 2 (*RUNX2*) and *SP7* mRNAs and of Runx2 and Sp7 proteins in the noncontact co-cultured periodontal ligament stem cell (PDLSC)/human umbilical vein endothelial cell (HUVEC) system under hypoxic exposure. Levels of *RUNX2* mRNA (A) and *SP7* mRNA (B), and expression of Runx2 protein (E) and Sp7 protein (F), after various time-periods of hypoxic treatment. * $p < 0.05$ vs. control. (C, D, G, H) Comparison of the co-culture group with the PDLSC group, at each time-point, for expression of *RUNX2* mRNA (C), *SP7* mRNA (D), Runx2 protein (G) and Sp7 protein (H), respectively. * $p < 0.05$ between the two groups.

time-points ($p < 0.05$) (Fig. 4C). The concentration of Runx2 protein was significantly increased by hypoxia at all time-points ($p < 0.05$). It transiently increased at 1 h, by 2.15-fold, after hypoxic exposure, then remained higher than the control throughout the experiment (Fig. 4E). When comparing the co-culture group with the PDLSC group, expression of the Runx2 protein was increased significantly at all time-points ($p < 0.05$) (Fig. 4G).

Hypoxic treatment significantly augmented the expression of *SP7* mRNA compared with the control at all time-points ($p < 0.05$). The level of *SP7* mRNA was very low in unstimulated cells, was induced prominently, by 2.789-fold, after 1 h of hypoxic treatment, and peaked at 3 h with a 2.848-fold increase; the expression level decreased at subsequent time-points but still remained higher than levels in the untreated control group ($p < 0.05$) (Fig. 4B). Comparison of the co-culture group with the PDLSC group at each time-point showed that the expression of *SP7* mRNA was increased by 2.266-, 3.945-, 1.445-, 0.776-, 1.064-, and 1.605-fold, respectively, with the results being significantly different at 1, 3 and 6 h ($p < 0.05$) (Fig. 4D). The amount of Sp7 protein was significantly increased at 1 h by 2.47-fold, then remained significantly higher than the control at 3, 6 and 12 h, finally peaking at 24 h

with a 4.38-fold increase ($p < 0.05$) (Fig. 4F). Comparison of the co-culture group with the PDLSC group at each time-point showed that the expression of Sp7 protein was increased significantly at all time-points ($p < 0.05$) (Fig. 4H).

Hypoxia enhances mineralized nodule formation in noncontact co-cultured PDLSCs

In order to understand more clearly the effect of hypoxia on the mineralization activity of the noncontact co-cultured PDLSCs *in vitro*, we carried out modified von Kossa's silver nitrate staining experiments to measure calcium nodule formation of PDLSCs after different time-periods of hypoxic treatment. The results indicated that hypoxia further augmented the formation of calcium nodules by noncontact co-cultured PDLSCs at all time-points, with a maximal density of 55.72 ± 2.95 nodules/cm² (Fig. 5).

Hypoxia up-regulates the ERK1/2 and p38 MAPK levels in PDLSCs

To investigate whether ERK1/2 and p38 MAPK signals were involved in osteogenesis of noncontact co-cultured PDLSCs under hypoxia, the activities of ERK1/2 and p38 MAPK were examined by western blotting. The results showed that both ERK1/2 and p38 MAPK were activated by hypoxia.

Hypoxic treatment led to a lagged and sustained phosphorylation of ERK1/2, which showed a moderate increase at 1 h and 3 h, and peaked at 6 h, but then showed a gradually decrease subsequently and remained higher than the control (Fig. 6A). In contrast, p38 MAPK subtype was activated in a relatively rapid and transient manner. The activity of phosphorylated p38 MAPK was immediately up-regulated at 1 h, then gradually decreased before increasing again as osteogenesis proceeded, reaching a second peak at 7 h, followed by a sharp decrease at 24h (Fig. 6B).

Concentration-dependent effect of MAPK inhibitors on ERK1/2 and p38 MAPK activity

ERK1/2 and p38 MAPK activities were examined after treatment of PDLSCs with MAPK inhibitors for 12 h. The results showed that both PD98059 and SB203580 regulated the kinase activities in a concentration-dependent manner. When PD98059 was used at 5 μ M, the Ap-ERK1/2/AERK1/2 ratio was decreased to about 1/3 of the control levels and the Ap-ERK1/2/AERK1/2 ratio decreased to 1/8 and 1/10 when PD98059 was used at final concentrations of 10 and 20 μ M, respectively (data not shown). This indicated that 10 μ M PD98059 was more effective at inhibiting MEK/ERK activity than 5 μ M, but had similar effects to 20 μ M under the

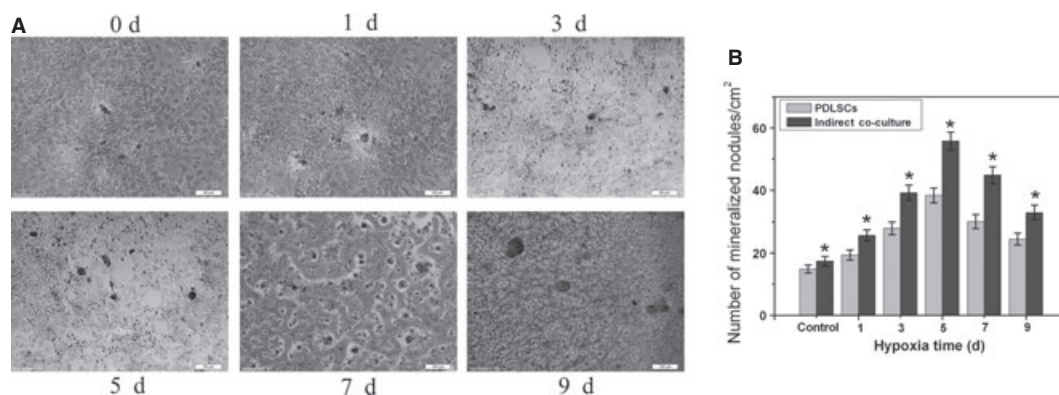


Fig. 5. Mineralized nodule formation of noncontact co-cultured periodontal ligament stem cells (PDLSCs) under hypoxic exposure. (A) Microscopy observation of mineralized nodule formation by the noncontact co-cultured PDLSCs after various time-periods (0, 6, 12, 24, 48, and 72 h) of hypoxic treatment. Scale bars = 50 μ m. (B) Quantitation of the density of mineralized nodules formed in PDLSCs and noncontact co-cultured PDLSCs after various time-periods of hypoxic treatment. Each bar represents the mean value of the number of mineralized nodules ($n = 5$ for each time-point) obtained from three experiments carried out in parallel. * $p < 0.05$ vs. control.

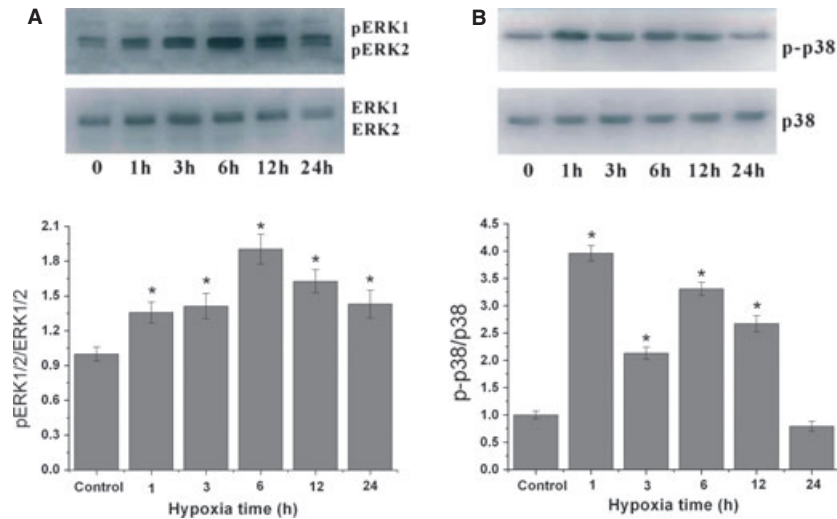


Fig. 6. Activity of ERK1/2 and p38 MAPK under hypoxic exposure. Expression of pERK1/2 and ERK1/2 proteins (A) and of p-p38 MAPK and p38 MAPK proteins (B) after various time-periods of hypoxic treatment. The kinase activity was analyzed by the band intensity ratio of p-ERK1/2 and ERK1/2, and of p-p38 MAPK and p38 MAPK and is presented in the histograms. * $p < 0.05$ vs. control.

current experimental conditions. Likewise, when SB203580 was provided at final concentrations of 1, 3 and 9 μM , the Ap-p38/Ap38 MAPK level decreased to 51%, 15% and 10%, respectively. Therefore, in the following pharmacological inhibition study, PD98059 and SB203580 were used at final concentrations of 10 and 3 μM respectively.

MAPK inhibitors exert an inhibitory effect on hypoxia-induced osteogenesis of noncontact co-cultured PDLSCs

To investigate whether MAPK signaling pathways are involved in the up-regulation of osteogenic-related genes (*HIF-1 α* , ALP, Runx2, Sp7, PGE₂ and VEGF) under hypoxic conditions, PDLSCs were pretreated with 10 μM PD98059 (ERK inhibitor) or 3 μM SB203580 (p38 MAPK inhibitor) under hypoxia for 6 h before noncontact co-culture with HUVECs for the indicated periods of time. First of all, the ALP activity assay was carried out, and the results showed that SB203580 significantly attenuated the hypoxia-induced ALP activation by about 65% while PD98059 moderately reversed the induction by nearly 40% ($p < 0.05$) (Fig. 7A). Then, qRT-PCR experiments were performed to determine the mRNA levels of *HIF1 α* ,

RUNX2 and *SP7*. We found that the augmented expression of *HIF1 α* and osteogenic-specific genes (*RUNX2* and *SP7*) by 6 h of hypoxic treatment was significantly blocked by PD98059 and SB203580 ($p < 0.05$), while SB203580 exerted a relatively stronger effect than PD98059 (Fig. 7B–D). Moreover, 10 μM PD98059 and 3 μM SB203580 significantly abolished the hypoxia-induced production of PGE₂ and VEGF ($p < 0.05$) (Fig. 7E,F).

Discussion

The present study employed a three-gas modular hypoxic incubator and a Transwell cell co-culture system to explore the impact of hypoxia on the osteogenic differentiation and mineralization of PDLSCs, noncontact co-cultured with HUVECs, at cellular and molecular levels. We found, for the first time, that exposure of co-cultured PDLSCs to hypoxia (2% O₂) led to further increased levels of PGE₂ and VEGF in the supernatants of the co-culture system, and to the additional up-regulation of osteoblastic differentiation markers (ALP, Runx2 and Sp7), at transcriptional and protein levels, as well as enhanced mineralized nodule formation in PDLSCs, compared with PDLSCs cultured alone. The study also demonstrated that ERK1/2 and p38 MAPK showed

different patterns of activation by hypoxia in PDLSCs during osteogenesis, and the two MAPK subtypes played complex roles in gene transcription and expression of the osteogenesis-specific markers/regulators *HIF-1 α* , ALP, Runx2, Sp7, PGE₂ and VEGF.

Angiogenesis is an essential component of skeletal development and is tightly coupled with osteogenesis during bone regeneration (28). It modulates bone formation by the production of growth factors with the ability to regulate osteoblastic activity and to recruit stem cells and stimulate their orientation to the osteoblastic lineage (29). MSCs, which produce osteoblasts, are found in their niche around the microvasculature, which contains large numbers of vascular ECs (17,18). During bone formation or remodeling, there is crosstalk between ECs and osteoprogenitors/osteoblasts within the vascular niche (30). MSCs in the developing stroma elicit angiogenic signals to recruit new blood vessels into bone. Reciprocal signals, probably emanating from the incoming vascular endothelium, stimulate stem-cell specification (31). The nature of the cellular and molecular mechanisms responsible for coupling angiogenesis and osteogenesis during bone formation remains poorly understood, but a primary driving force is tissue hypoxia. The *HIF-1 α* pathway has been

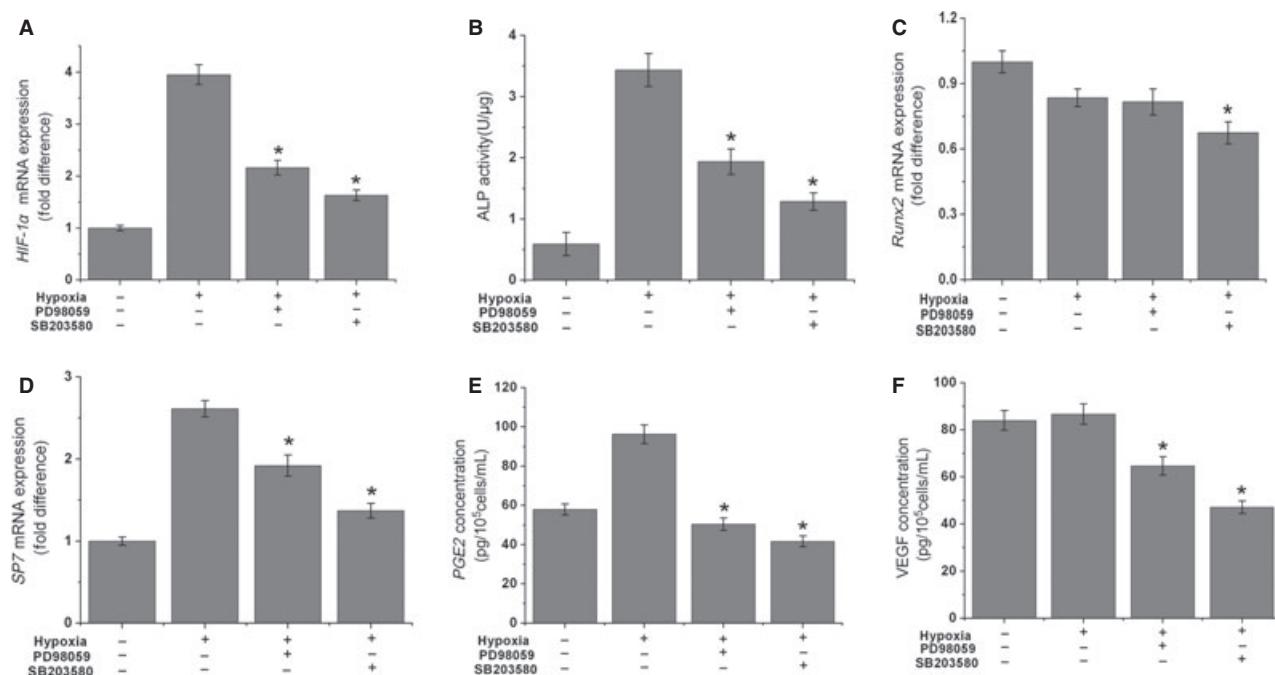


Fig. 7. Effects of PD98059 and SB203580 on alkaline phosphatase (ALP) activity, on the concentrations of vascular endothelial growth factor (VEGF) and prostaglandin E₂ (PGE₂), and on the expression of hypoxia-inducible factor-1 α (*HIF1 α*), runt-related transcription factor 2 (*RUNX2*) and *SP7* mRNAs. Periodontal ligament stem cells (PDLSCs) were treated with 10 μ M of PD98059 or with 3 μ M of SB203580 under hypoxia for 6 h, the ALP activity was assessed, the concentrations of VEGF and PGE₂ were determined and the levels of expression of *HIF1 α* , *RUNX2* and *SP7* mRNAs were examined by quantitative RT-PCR. (A) *HIF1 α* mRNA, (B) ALP activity, (C) *RUNX2* mRNA; (D) *SP7* mRNA, (E) PGE₂ concentration and (F) VEGF concentration. * $p < 0.05$ vs. the hypoxic group.

demonstrated to be critical in this process as a result of enhanced angiogenic activity, which is mediated by elevated levels of VEGF in HIF-1 α -overexpressing osteoblasts (32). Furthermore, HIF-1 may influence the development of the osteoblast-vascular niche (33). However, there have been no reports regarding the effects of vascular ECs on the osteogenic differentiation of noncontact co-cultured PDLSCs under hypoxia, and we further reveal the involvement of MEK/ERK and p38 MAPK pathways in the process.

Although the noncontact co-culture system could not completely mimic the spatial relationship between the two types of cells during periodontal regeneration, it enabled real-time regulation of HUVECs on PDLSCs and avoided the difficulty of cellular and molecular analyses in a direct co-culture system (34). The results demonstrated the differentiation of increased numbers of PDLSCs into osteoblasts and mineralization in the noncontact

co-culture system under hypoxia, compared with PDLSCs cultured alone. Nevertheless, Clarkin *et al.* (35) provided evidence that direct contact between osteoblasts and ECs resulted in the suppression of osteoblast ALP activity, by the loss of VEGF sensitivity and attenuation of VEGF signaling by endogenous prostaglandins.

Abundant evidence indicates that the vasculature plays an active and important role in numerous skeletal pathologies, and pro-angiogenic VEGF-mediated signaling is tightly associated with bone regeneration and remodeling (35). Various previous studies have provided firm evidence for augmented osteoblastic differentiation, and for EC proliferation, migration and tube formation in co-culture of osteoprogenitor cells and ECs (22,36,37). Reciprocity of osteoblasts and vascular ECs by VEGF or direct action has been indicated as an important mechanism underlying bone remodeling (38,39). Moreover, osteoblast-derived VEGF has been identified

to enhance primary angiogenesis events and osteoblastic differentiation through chemoattractive/proangiogenic effects in an autocrine/paracrine manner; meanwhile, inhibition of VEGF receptors reduced the co-culture-stimulated osteoblastic phenotype (22). Interestingly, exogenous VEGF was deduced to have a positive effect on cell proliferation in the co-culture system, whereas this factor alone did not affect EC migration in isolated cultures (22,36). Therefore, VEGF appeared to be one (but not exclusively) of the soluble factors that have a crucial role in co-culture-stimulated cell rearrangement and osteoblastic differentiation. Similarly to PGE₂, our investigation showed additional hypoxia-induced augmentation of VEGF synthesis and release by PDLSCs and HUVECs, compared with PDLSCs cultured alone under hypoxia. Therefore, VEGF derived from PDLSCs or HUVECs is likely to exert a paracrine effect on the function of vascular ECs or PDLSCs in periodontal tissue remodeling during

OTM. Our studies also suggested the proximity of PDLSCs to ECs as a critical factor in determining how PGE₂ and VEGF contribute to this vital intercellular communication.

Prostaglandins, ubiquitously present in mammalian tissues, were proposed to act as typical intercellular mediators that can provide both a localized response and signal amplification necessary for bone metabolism (40,41). There is evidence to suggest that bone remodeling induced by mechanical forces *in vivo* is prostaglandin-mediated (42). Moreover, PGE₂ is one of the most potent bone resorbers *in vitro* (43). Several studies have shown that osteoblasts cultured *in vitro* produce VEGF in response to a range of factors, including PGE₂ and HIF-1 α , and that this VEGF acts predominantly in a paracrine manner, ensuring efficient communication with ECs (33,34). In contrast, blockade of endogenous cyclooxygenase 2 activity with NS398, which blocks the production of a range of prostanoids, strongly inhibited VEGF-induced EC proliferation in a co-culture system of HUVECs and osteoblasts (35). The relationship that exists between VEGF and prostaglandins has been postulated to play a positive-feedback role in the control of angiogenesis (44,45). However, no reports are currently available regarding the effects of hypoxia on the secretion of PGE₂ in a noncontact co-cultured system of PDLSCs and HUVECs. In the present study, we observed further increased synthesis and release of PGE₂, in a time-dependent manner, by PDLSCs and HUVECs that were stimulated by hypoxia, compared with PDLSCs cultured alone under hypoxia. We identified a synergistic effect of both hypoxic exposure and noncontact co-culture with HUVECs on the enhancement of PGE₂ release. However, a study has reported that under conditions of closely direct contact of osteoblasts and ECs, pharmacological blockade of endogenous cyclooxygenase 2 activity augmented EC-driven increases in osteoblast differentiation, which could be reversed by co-incubation with Prostaglandins H₂ (37). This indicates that the spatial relationship of osteo-

blasts and ECs may affect the way they communicate, and the mechanisms involved need further investigation.

The MAPK family includes p38 MAPK, JNK and ERK (46). Several lines of evidence imply that MAPK signaling is essential for osteoblast differentiation and osteoblast-related gene expression (47,48). There are also reports suggesting that MAPK pathways play critical roles in directing MSC commitment to the osteogenic lineage (49). Among the three pathways of the MAPK superfamily, ERK signaling is involved in driving extracellular matrix-induced osteogenic differentiation of MSC via Runx2 phosphorylation, while p38 MAPK is responsible for environmental stimuli, such as oxidative stress (48,50). In myocardium, ischemic injury activates p38 MAPK and nuclear factor-kappaB, and three kinases of MAPK are deduced to be up-regulated after cerebral hypoxia/ischemia (51). Previous data also indicated that MAPK pathways can activate and phosphorylate Runx2 *in vitro*, which subsequently initiates the transcription of osteogenesis-specific genes, including ALP (51). Moreover, the phenomenon that activation of MAPKs depends on the nature of the stimuli and on the cell type, strongly suggests that ERK and p38 MAPK pathways display distinct spatio-temporal patterns of activation in response to a hypoxic stress (52). Therefore, we hypothesized that hypoxia may serve as a stimuli on noncontact co-cultured PDLSCs to activate the MAPK signaling pathway in the cells and induce their preferential osteogenic differentiation.

Our investigation showed that phosphorylation of ERK1/2 and p38 MAPK signals developed in different patterns. Hypoxic treatment resulted in a slow and lasting phosphorylation of ERK1/2, whereas p38 MAPK signals was phosphorylated in a relatively rapid and transient way, suggesting that the p38 MAPK subtype is more sensitive to oxidative stress. Similar results were documented in a study observing a transient and early increase in the p38 MAPK and Stress activated protein kinase/JNK levels of MSCs under 2.2% hypoxic conditions (51). Additional studies have shown that apart

from the p38 MAPK signal, ERK is also activated by hypoxia and ischemia and may play an important role in the adaptive response to hypoxia (53).

To sum up, one hypoxia-responsive gene (*HIF1 α*), three osteogenesis-specific genes (*ALP*, *RUNX2* and *SP7*), two proangiogenic autocrine/paracrine factors (PGE₂ and VEGF) and two MAPK subtypes (ERK and p38 MAPK) of PDLSCs or the noncontact co-cultured system were confirmed to be significantly enhanced under hypoxia. In addition to the well-known MAPK-dependent regulation of Runx2 and Sp7, the MAPK family has also been reported to play an important role in oxidant-mediated HIF-1-dependent VEGF expression (54). Taken together, these observations prompted us to explore in greater detail whether the expression profile of the above genes are affected by MAPK inhibitors in noncontact co-cultured PDLSCs after hypoxic treatment. The results proved that PD98059 (ERK inhibitor) and SB203580 (p38 MAPK inhibitor) significantly abrogated the hypoxia-induced augmentation of *HIF1 α* , *ALP*, *RUNX2*, *SP7*, *PGE2* and *VEGF* genes, providing the first indication that the enhanced osteogenic differentiation and paracrine function of noncontact co-cultured PDLSCs under hypoxia were mediated by MEK/ERK and p38 MAPK signaling activation (Fig. 7). Furthermore, the findings that the inhibitory effects of SB203580 were stronger than PD98059 for all the osteogenesis-related genes, together with the evidence that p38 MAPK responded to hypoxia in a more rapid and vigorous manner than ERK, indicates a more important role for p38 MAPK in hypoxia-induced PDLSC osteogenesis and in PGE₂ and VEGF release.

In conclusion, exposure of noncontact co-cultured PDLSCs to hypoxia significantly activated MEK/ERK and p38 MAPK signaling cascades, which stimulated the expression of transcriptional factors Runx2 and Sp7, and subsequently up-regulated the osteogenesis regulatory genes *ALP*, *PGE2* and *VEGF*, and finally the long-term mineralized nodule formation. Our studies may confirm a paracrine EC-mediated

effect of PGE₂ and VEGF on differentiation of PDLSCs into osteoblasts and support a model in which PGE₂ and VEGF may facilitate this unidirectional PDLSC–EC communication. These findings may offer novel regimes for modulating periodontal remodeling through controlling the differentiation of PDLSCs into osteoblasts and the functions of ECs. Innovative strategies, including the application of hypoxia-mimicking agents to create a hypoxic environment that favors regenerative attempts, can also be incorporated into traditional strategies with tremendous future potential.

Acknowledgements

This work was supported by grants from National Undergraduates Innovative Experimentation Project (NO. 2009009).

Reference

- Paris S, Denis H, Delaive E. Up-regulation of 94-kDa glucose-regulated protein by hypoxia-inducible factor-1 in human endothelial cells in response to hypoxia. *FEBS Lett* 2005;**579**:105–114.
- Sluimer JC, Gasc JM, vanWanroij JL *et al.* Hypoxia, hypoxia-inducible transcription factor, and macrophages in human atherosclerotic plaques are correlated with intraplaque angiogenesis. *J Am Coll Cardiol* 2008;**51**:1258–1265.
- Salim A, Nacamuli RP, Morgan EF. Transient Changes in Oxygen Tension Inhibit Osteogenic Differentiation and Runx2 Expression in Osteoblasts. *J Biol Chem* 2004;**279**:40007–40016.
- Flamant L, Toffoli S, Raes M, Michiels C. Hypoxia regulates inflammatory gene expression in endothelial cells. *Exp Cell Res* 2009;**315**:733–747.
- Pradeep AR, Prapulla DV, Sharma A, Sujatha PB. Gingival crevicular fluid and serum vascular endothelial growth factor: their relationship in periodontal health, disease and after treatment. *Cytokine* 2011;**54**:200–204.
- Jonsdottir SH, Giesen EB, Maltha JC. Biomechanical behaviour of the periodontal ligament of the beagle dog during the first 5 hours of orthodontic force application. *Eur J Orthod* 2006;**28**:547–552.
- Peschkowa LW, Warawa GN, Orlawa OL. New concept on the mechanism of hypoxia in case of periodontitis. *Stomatol DDR* 1990;**40**:67–69.
- Ng KT, Li JP, Ng KM, Tipoe GL, Leung WK, Fung ML. Expression of hypoxia-inducible factor-1 α in human periodontal tissue. *J Periodontol* 2011;**82**:136–141.
- Motohira H, Hayashi J, Tatsumi J, Tajima M, Sakagami H, Shin K. Hypoxia and reoxygenation augment bone-resorbing factor production from human periodontal ligament cells. *J Periodontol* 2007;**78**:1803–1809.
- Ben-Av P, Crofford LJ, Wilder RL, Hla T. Induction of vascular endothelial growth factor expression in synovial fibroblasts by prostaglandin E and interleukin-1: a potential mechanism for inflammatory angiogenesis. *FEBS Lett* 1995;**372**:83–87.
- Carmeliet P, Ferreira V, Breier G. Abnormal blood vessel development and lethality in embryos lacking a single VEGF allele. *Nature* 1996;**380**:435–439.
- Yun Z, Maecker HL, Johnson RS, Giaccia AJ. Inhibition of PPAR gamma 2 gene expression by the HIF-1-regulated gene DEC1/Stra13: a mechanism for regulation of adipogenesis by hypoxia. *Dev Cell* 2002;**2**:331–341.
- Riddle RC, Khatri R, Schipani E, Clemens TL. Role of hypoxia-inducible factor-1 α in angiogenic-osteogenic coupling. *J Mol Med (Berl)* 2009;**87**:583–590.
- Mandracchia VJ, Nelson SC, Barp EA. Current concepts of bone healing. *Clin Pediatr Med Surg* 2001;**18**:55–77.
- Seo BM, Miura M, Gronthos S *et al.* Investigation of multipotent postnatal stem cells from human periodontal ligament. *Lancet* 2004;**364**:149–155.
- Wu L, Wei X, Ling J *et al.* Early osteogenic differential protein profile detected by proteomic analysis in human periodontal ligament cells. *J Periodont Res* 2009;**44**:645–656.
- Spradling A, Drummond-Barbosa D, Kai T. Stem cells find their niche. *Nature* 2001;**414**:98–104.
- Scadden DT. The stem-cell niche as an entity of action. *Nature* 2006;**441**:1075–1079.
- Moore KA, Lemischka IR. Stem cells and their niches. *Science* 2006;**311**:1880–1885.
- Gould TR, Melcher AH, Brunette DM. Migration and division of progenitor cell populations in periodontal ligament after wounding. *J Periodontol Res* 1980;**15**:20–42.
- McCulloch CA. Progenitor cell populations in the periodontal ligament of mice. *Anat Rec* 1985;**211**:258–262.
- Grellier M, Ferreira-Tojais N, Bourget C, Bareille R, Guillemot F, Amedee J. Role of Vascular Endothelial Growth Factor in the Communication Between Human Osteoprogenitors and Endothelial Cells. *J Cell Biochem* 2009;**106**:390–398.
- Calabrese C, Poppleton H, Kocak M *et al.* A Perivascular Niche for Brain Tumor Stem Cells. *Cancer Cell* 2007;**11**:69–82.
- Louissaint A Jr, Rao S, Leventhal C, Goldman SA. Coordinated interaction of neurogenesis and angiogenesis in the adult songbird brain. *Neuron* 2002;**34**:945–960.
- Yoshida S, Sukeno M, Nabeshima Y. A vasculature-associated niche for undifferentiated spermatogonia in the mouse testis. *Science* 2007;**317**:1722–1726.
- Carrancio S, Lopez-Holgado N, Sanchez-Guijo FM *et al.* Optimization of mesenchymal stem cell expansion procedures by cell separation and culture conditions modification. *Exp Hematol* 2008;**36**:1014–1021.
- Gronthos S, Mankani M, Brahimi J, Robey PG, Shi S. Postnatal human dental pulp stem cells (DPSCs) in vitro and in vivo. *Proc Natl Acad Sci USA* 2000;**97**:13625–13630.
- Brandi ML, Collin-Osdoby P. Vascular biology and the skeleton. *J Bone Miner Res* 2006;**21**:183–192.
- Fiedler J, Leucht F, Waltenberger J, Dehio C, Brenner RE. VEGF-A and PIGF-1 stimulate chemotactic migration of human mesenchymal progenitor cells. *Biochem Biophys Res Commun* 2005;**334**:561–568.
- Ferguson C, Alpern E, Miclau T, Helms JA. Common molecular pathways in skeletal morphogenesis and repair. *Mech Dev* 1999;**87**:57–66.
- Gerber HP, Ferrara N. Angiogenesis and bone growth. *Trends Cardiovasc Med* 2000;**10**:223–228.
- Wang Y, Wan C, Deng L *et al.* The hypoxia-inducible factor alpha pathway couples angiogenesis to osteogenesis during skeletal development. *J Clin Invest* 2007;**117**:1616–1626.
- Wan C, Gilbert SR, Wang Y *et al.* Activation of the hypoxia-inducible factor-1 α pathway accelerates bone regeneration. *Proc Natl Acad Sci USA* 2008;**105**:686–691.
- Clarkin CE, Emery RJ, Pitsillides AA, Wheeler-Jones CP. Evaluation of VEGF-Mediated Signaling in Primary Human Cells Reveals a Paracrine Action for VEGF in Osteoblast-Mediated Crosstalk to Endothelial Cells. *J Cell Physiol* 2008;**214**:537–544.
- Clarkin CE, Garonna E, Pitsillides AA, Wheeler-Jones CPD. Heterotypic contact reveals a COX-2-mediated suppression of osteoblast differentiation by endothelial cells: a negative modulatory role for prostanooids in VEGF-mediated cell: cell communication? *Exp Cell Res* 2008;**314**:3152–3161.
- Villars F, Bordenave L, Bareille R, Amedee J. Effect of human endothelial cells on

- human bone marrow stromal cell phenotype: role of VEGF? *J Cell Biochem* 2000;**79**:672–685.
37. Guillotin B, Bourget C, Remy-Zolgadri M *et al*. Human primary endothelial cells stimulate human osteoprogenitor cell differentiation. *Cell Physiol Biochem* 2004;**14**:325–332.
 38. Midy V, Plouet J. Vasculotropin/vascular endothelial growth factor induces differentiation of cultured osteoblasts. *Biochem Biophys Res Commun* 1994;**199**:380–386.
 39. Villanueva JE, Nimni ME. Promotion of calvarial cell osteogenesis by endothelial cells. *J Bone Miner Res* 1990;**5**:733–739.
 40. Hassid A. Regulation of prostaglandin biosynthesis in cultured cells. *Am J Physiol* 1982;**243**:C205–C211.
 41. Raisz LG, Martin TJ. Prostaglandins in bone and mineral metabolism. In: Peck WA, eds. *Bone and Mineral Research Annual II*. Excerpta Medica: Amsterdam, 1983: 286–310.
 42. Yamasaki K, Miura F, Suda T. Prostaglandin as a mediator of bone resorption induced by experimental tooth movement in monkeys. *J Dent Res* 1980;**59**:1636–1642.
 43. Tashjian AH Jr, Tice JE, Sides K. Biological activities of prostaglandin analogues and metabolites on bone in organ culture. *Nature* 1977;**266**:645–646.
 44. Sakurai T, Tamura K, Kogo H. Vascular endothelial growth factor increases messenger RNAs encoding cyclooxygenase-II and membrane-associated prostaglandin E synthase in rat luteal cells. *J Endocrinol* 2004;**183**:527–533.
 45. Tamura M, Sebastian S, Gurates B, Yang S, Fang Z, Bulun SE. Vascular endothelial growth factor up-regulates cyclooxygenase-2 expression in human endothelial cells. *J Clin Endocrinol Metab* 2002;**87**:3504–3507.
 46. Raman M, Chen W, Cobb MH. Differential regulation and properties of MAPKs. *Oncogene* 2007;**26**:3100–3112.
 47. Lou J, Tu Y, Li S, Manske PR. Involvement of ERK in BMP-2 induced osteoblastic differentiation of mesenchymal progenitor cell line C3H10T1/2. *Biochem Biophys Res Commun* 2000;**268**:757–762.
 48. Schmidt C, Pommerenke H, Durr F, Nebe B, Rychly J. Mechanical stressing of integrin receptors induces enhanced tyrosine phosphorylation of cytoskeletonally anchored proteins. *J Biol Chem* 1998;**273**:5081–5085.
 49. New L, Han J. The p38 MAP kinase pathway and its biological function. *Trends Cardiovasc Med* 1998;**8**:220–229.
 50. Alessandrini A, Namura S, Moskowitz MA, Bonventre JV. MEK1 protein kinase inhibition protects against damage resulting from focal cerebral ischemia. *Proc Natl Acad Sci USA* 1999;**96**:12866–12869.
 51. Lee SH, Lee YJ, Song CH, Ahn YK, Han HJ. Role of FAK phosphorylation in hypoxia-induced hMSCS migration: involvement of VEGF as well as MAPKS and eNOS pathways. *Am J Physiol Cell Physiol* 2010;**298**:C847–C856.
 52. Zarubin T, Han J. Activation and signaling of the p38 MAP kinase pathway. *Cell Res* 2005;**15**:11–18.
 53. Cox BD, Natarajan M, Stettner MR, Gladson CL. New concepts regarding focal adhesion kinase promotion of cell migration and proliferation. *J Cell Biochem* 2006;**99**:35–52.
 54. Mottet D, Michael G, Renard P, Ninane N, Raes M, Michiels C. Role of ERK and calcium in the hypoxia-induced activation of HIF-1. *J Cell Physiol* 1994;**194**:30–44.

This document is a scanned copy of a printed document. No warranty is given about the accuracy of the copy. Users should refer to the original published version of the material.